

# Topology optimisation method for crashworthiness design using Hybrid Cellular Automata and thin-walled ground structures

Stephan Hunkeler<sup>1</sup>, Fabian Duddeck<sup>2</sup> and Milan Rayamajhi<sup>1</sup>

<sup>1</sup>Queen Mary University of London, School of Engineering and Materials Science, London, UK

<sup>2</sup>Technische Universität München, FG Computational Mechanics, München, Germany

Crashworthiness is one of the most demanding design cases for vehicle structures. Until a few years ago, it was mainly addressed using trial and error approaches; but recently, automated structural optimisation for crashworthiness design got more and more popular. So far, most relevant applications use size or shape optimisation. Nevertheless, the ultimate way to achieve significant mass reduction is to use topology optimisation.

While topology optimisation for static mechanics is a well established field of research, applications to crashworthiness can be rarely found. Due to high non-linearity of crash simulation, classic topology optimisation methods cannot be applied directly to crashworthiness design. Therefore, alternative methods have been developed. This paper first presents the available methods for topology optimisation in crashworthiness design. A discussion of these methods highlights the opportunity to develop an alternative method which is detailed in the second section of this paper. Then two application examples are presented to showcase the interest and capabilities of this method.

## 1 Topology optimisation for crashworthiness design

Topology optimisation is well established for static mechanics or even electromechanical problems. Classic topology optimisation methods such as Solid Isotropic Material with Penalisation (SIMP) [1] rely on node-based sensitivities to perform the optimisation and the number of design variables is equal to the number of finite elements in the initial model. This is not adapted to crashworthiness design with explicit finite element simulation as computing sensitivities throughout the model would require an unrealistic amount of computations which are already expensive on their own. Alternative methods have been developed based on two principles. Firstly, the explicit finite element simulation can be replaced by a less expensive simulation method. Secondly, the classic topology optimisation method can be replaced by an alternative optimisation method usually reducing the number of design variables or a method which does not guarantee the optimality of its result. The main methods for topology optimisation in crashworthiness design are detailed in the next sections.

### 1.1 Equivalent Static Loads (ESL) based methods

The ESL methods are based on the fact that, under certain conditions, a fully dynamic non-linear crash simulation can be replaced by a series of consecutive linear simulations using static loads with the same deformation effects as the dynamic load. Two different forms of ESL methods should be distinguished using either global loads or node-based loads.

#### 1.1.1 *ESL and global static loads*

In the first method, global ESL are defined representing the interactions between the vehicle or component to optimise and the external elements involved in the crash (e.g. impactor, rigid wall). Different variants on this method can be found in literature. Volz [2, 3] presented a version of the method where the loads are defined using crash kinematics considerations. First the ratios of energy which should be absorbed by the different areas of the design domain are defined. Combining these different energy absorption targets and geometric considerations, force levels are derived with their time dependency. From these force levels, the ESL are defined and the multi load case static linear topology optimisation can be performed using classic methods.

Christensen [4] and Cavazzuti [5] presented different variants of the method using a single static load to represent the crash load.

### 1.1.2 Nodal based Equivalent Static Loads

This method, mostly developed by Park *et al.* [6, 7], defines the Equivalent Static Loads at the finite element level with artificial forces applied to each node of the model. This allows for a finer control of the model deformations but the effort to extract the loads is higher. Using a set of Equivalent Static Loads for each desired time step, the topology optimisation problem can be solved as a multi load case linear static topology optimisation problem.

An overview of the applications of these methods is given in [8], including both size and topology optimisation problems.

## 1.2 Ground Structure approach (GSA)

The ground structure approach consists in filling the design space with elementary macro-elements with a simplified crash behaviour and using different methods to remove and/or modify these macro-elements to reach an optimum design. Pedersen [9] proposed a ground structure composed of rectangular 2D beam elements with plastic hinges. Those elements can undergo large rotations and their main design variable is their cross-section dimension. The optimisation problem is solved using the analytical crash behaviour of these elements.

## 1.3 Graph-based method

This method, detailed in [10], is based on an abstract Graph representation of the structure, usually for 2D design spaces (such as the cross-section of longitudinal elements). The topology optimisation method is divided into two processes. An outer one where the topology level of the cross-section is iterated and an inner one where a shape optimisation is performed on the current topology level. After each shape optimisation result, the topology level of the structure is modified by adding or removing walls in the cross-section. This modification is made using heuristic rules which evaluate the contribution of the different walls of the cross-section and for instance delete the walls with low energy absorption or introduce new walls to support the walls with fast deformation.

## 1.4 Bi-directional Evolutionary Structural Optimisation (BESO)

In this method detailed in [11], the structure is designed to maximise the energy absorption efficiency while respecting some force and displacement constraints. After each finite element simulation, the elements of the model are assigned two sensitivity numbers, derived using an adjoint method. An adjoint equation is introduced in the calculation of the external work variation by adding a series of Lagrangian multipliers using the equilibrium of the non-linear equations. Using this adjoint equation the sensitivity numbers are derived. Those sensitivity numbers should allow to optimise for two different criteria, the energy absorbed per unit volume and the ratio of energy absorbed over the ideal energy absorption. Depending on the sensitivity numbers, elements will be either added or removed from the model while volume fraction of active elements in the model is adjusted in order to respect the force constraint. This process is iterated until an optimum is found.

## 1.5 Hybrid Cellular Automata (HCA)

HCA has been adapted for the synthesis of topologies in crashworthiness design by Patel [12] and then Mozumder [13]. It uses a regular grid of cells to cover the design space and update rules to modify the density of these cells depending on their Internal Energy Density (IED) (elastic and plastic deformation), and therefore derive a topology. The idea is to generate a homogeneous distribution of IED throughout the design space and to minimise the mass fraction of the design space while respecting the design constraints.

## 1.6 Discussion of the available methods

The methods listed above can be divided in two categories. On the first hand, methods such as node-based ESL, BESO and HCA which fill the design space with solid elements and derive bulk topologies. On the other hand, GSA and Graph-based method which derive thin-walled structures exploring only a subset of possible topologies.

As the first type of methods derives bulky structures, they may be better suited for design tasks where a high fraction of the initial design space should be filled with material. To derive structures with a low fraction of the initial design space, the discretisation should be really fine which strongly penalises the computation time. This first type of methods also usually involves some post-processing after the topology optimisation to transform the bulk structure into a thin-walled structure, more suitable for manufacturing. This process is not straight-forward as the interpreted structure can behave differently from the topology optimisation result.

On the other hand, methods deriving thin-walled structures are limited by the fact that they explore only a subset of all the possible solutions. In the GSA, the initial Ground Structure defines the possible solutions for the optimisation process. Similarly, the Graph-based method only explores a limited number of possible topologies.

In the next section, an alternative method for topology optimisation in crashworthiness is presented. This method tries to solve some of the shortcomings detailed previously.

## 2 Hybrid Cellular Automata applied to thin-walled structures

The method presented in this section proposes to generate 3D topologies with thin-walled structures combining the advantages of the HCA method and of a starting ground structure. The principles of the method are first introduced. Then, details of the algorithm are discussed. Eventually, an overview of the implementation of the method is given.

### 2.1 Hybrid Cellular Automata for Thin-Walled Structures (HCA-TWS)

#### 2.1.1 Coupling Hybrid Cellular Automata and thin-walled structures

The use of thin-walled structures directly in the optimisation allows to reproduce the specific deformation modes of these structures and to model self contacts or wall-to-wall contacts more easily. It also enables to skip the process of interpretation necessary when optimising with solid structures but designing for thin-walled structures. Compared with the classic HCA, the cells are not solid finite elements but small thin walls made of a number of shell finite elements. This is necessary with thin walls as their deformation modes do not produce homogeneous energy absorption for all shell elements. Higher energy absorption can be observed along the plastic hinge lines. With larger cells, the IED distribution can be more homogeneous amongst the cells.

The design variables of the algorithm are not the density of the finite elements as in the classic HCA but the thickness of the walls. The IED of each cell is still the corresponding output value.

#### 2.1.2 Space filling with thin walls

The question of space filling is crucial for HCA-TWS. For 3D design spaces, the space filling is a cubic honeycomb (in the mathematical sense, see Fig. 1) to allow for a regular space filling. This regular space filling is the condition to use the HCA method with requires a regular grid of cells. For 2D cases (e.g. extruded structures), the space filling is a square tiling (see Fig. 2, left) and can be enriched with diagonal elements by superimposing two other square fillings rotated by  $\pm 45$  degrees (see Fig. 2,

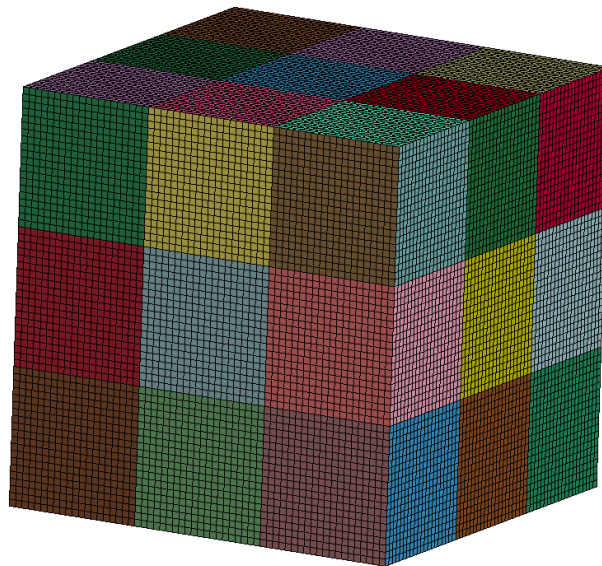


Figure 1: Meshed cells for cubic space filling.

right).

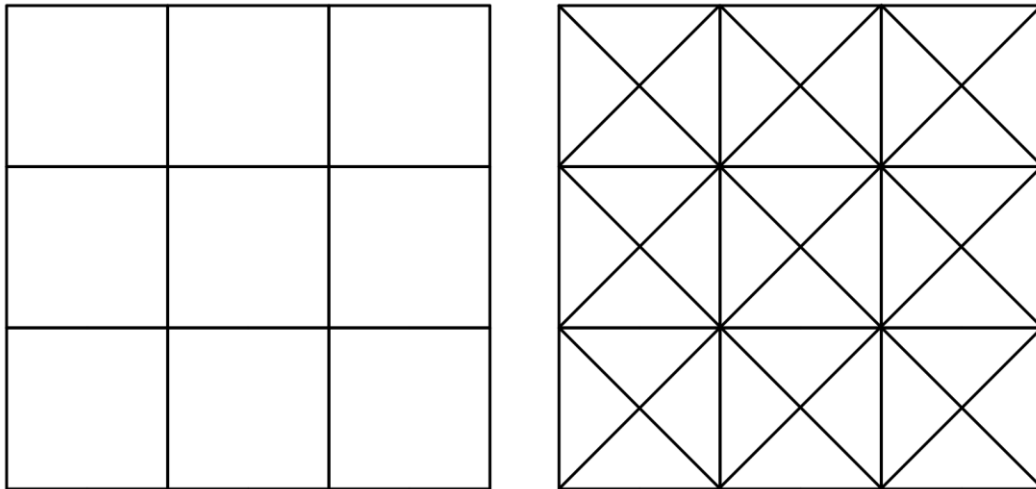


Figure 2: 2D square (left) and diagonal enriched (right) space filling.

### 2.1.3 Neighbourhood

The update rules for the cells use the output values of a given cell and its neighbouring cells. The neighbourhood also gives information on how cells interact with each other and ensures continuity in the structure. Defining neighbourhoods for thin macro elements is not necessarily trivial. Five different types of neighbourhoods for 3D space fillings are proposed in Fig. 3. Three different types of neighbourhoods for 2D space fillings are proposed in Fig. 4.



Figure 3: 3D neighbourhoods, empty, plane von Neumann, plane Moore, von Neumann, Moore.

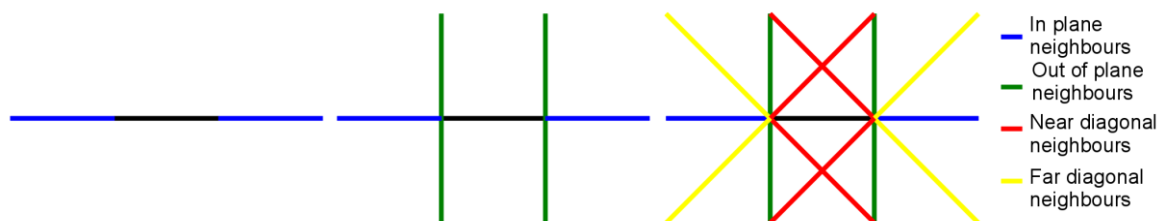


Figure 4: 2D neighbourhoods, plane (left), von Neumann (centre) and full diagonal (right).

### 2.1.4 Global performance objective and constraints

The HCA algorithm seeks the best material distribution to ensure a homogeneous IED distribution. With the macro cells used in HCATWS, it is easier to reach the same IED level between two cells than between two finite elements as in the classic HCA approaches.

Different design constraints (maximum displacement, maximum reaction force, force displacement curve) can be used in HCATWS. As in classic HCA, they are enforced by modifying the mass fraction target of the design space. The mass fraction is therefore chosen as low as possible while respecting the design constraint.

In some cases, it is desirable to finely tune the kinematics of the deformation. This can be done using different methods, with different levels of complexity. Defining sub-spaces with the design space, different acquisition times can be used for the IED or different IED setpoints can be used to control the kinematics of the crash.

### 2.1.5 Algorithm overview

Fig. 5 presents the organisation of the algorithm which is largely inspired by the classic HCA implementations [12,13]. Notations are clarified in the next paragraphs.

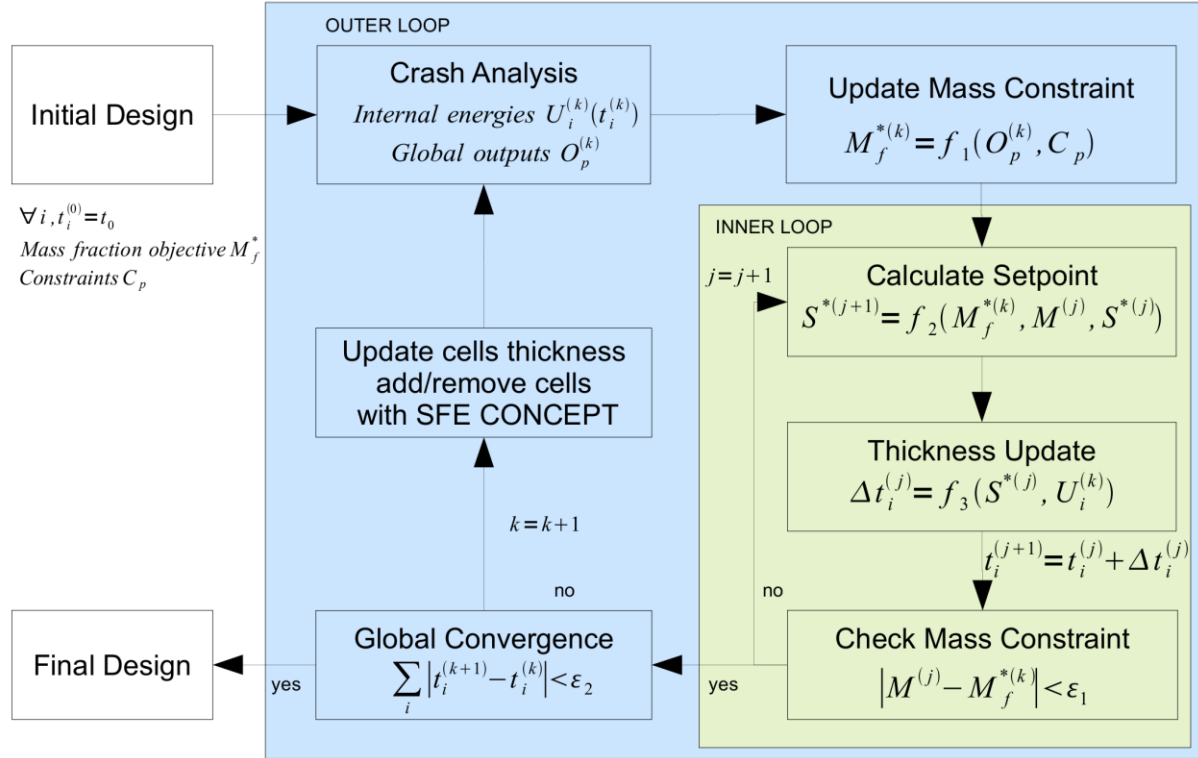


Figure 5: Algorithm overview.

## 2.2 Details of the algorithm

### 2.2.1 Design constraint

The design constraint presented here is the maximum displacement allowed. As discussed previously, other constraints can be implemented under the same principle. Given the maximum displacement allowed  $d_{max}$  and the displacement output at iteration  $k$ ,  $d_{out}^{(k)}$ , the displacement deviation  $\varepsilon_d^{(k)}$  is defined by:

$$\varepsilon_d^{(k)} = \frac{d_{out}^{(k)} - d_{max}}{d_{max}}. \quad (1)$$

The mass fraction objective (defined as the mass objective divided by the initial mass) for iteration  $k + 1$  is updated using the following equation:

$$M_f^{(k+1)} = \max(M_{f,min}, M_f^{(k)} + \Delta M_f^{(k)}) \quad (2)$$

Where  $M_{f,min}$  is the minimum mass fraction value and  $\Delta M_f^{(k)}$  is the mass fraction change defined as:

$$\Delta M_f^{(k)} = \min(\Delta M_{f,max}^{(k)}, \max(-\Delta M_{f,max}^{(k)}, \lambda_{\Delta M_f}^{(k)} \times \varepsilon_d^{(k)})) \quad (3)$$

$\lambda_{\Delta M_f}^{(k)}$  is the current mass fraction change modulation factor which regulates the mass fraction change speed and  $\Delta M_{f,max}^{(k)}$  is a decreasing function of the iteration  $k$  and parameters  $\eta$  and  $\tau$  defined as:

$$\Delta M_{f,max}^{(k)} = \max\left(\Delta M_{f,\eta} \times \exp\left(\frac{-k}{\tau}\right) \times M_f^{(k)}\right). \quad (4)$$

### 2.2.2 Setpoint update

The IED setpoint is updated within the "inner loop" (cf. Fig. 5) until the mass constraint of the next iteration is respected. For each step  $j$  of the "inner loop", the setpoint  $S^{(j,k)}$  is given by:

$$S^{(j+1,k)} = \min \left( S_{max}, \max \left( S_{min}, S^{(j,k)} \times \frac{mfc^{(j)}}{M_f^{(k+1)}} \right) \right) \quad (5)$$

Where  $mfc^{(j)}$  is the actual mass fraction at step  $j$  and  $S_{min}$  and  $S_{max}$  are the IED setpoint limit values.

### 2.2.3 Cells update rule

The update rule is inspired from both the work on HCA for crashworthiness design presented in [12] and from the work on HCA for static topology optimisation presented in [14]. It uses separate contributions from each of the neighbouring cells and accounts for the discrepancies between the setpoint and the IED levels of each neighbour. The thickness change  $\delta t_i^{(j,k)}$  for cell  $i$  is defined as:

$$\delta t_i^{(j,k)} = \min \left( \delta t_{max}, \max \left( -\delta t_{max}, \sum_{q=0}^{n_i} \alpha_q^{(j,k)} \right) \right) \quad (6)$$

Where  $\alpha_q^{(j,k)}$  is the contribution of cell  $q$ , defined as:

$$\alpha_q^{(j,k)} = \sum_{u=1}^{c_q} \zeta \times \chi_{P_u} \left( U_q^{(k)} \right) - \sum_{u=1}^{c_q} \zeta \times \chi_{M_u} \left( U_q^{(k)} \right) \quad (7)$$

$$\text{where } P_u = \left[ S^{(j,k)} + b_u \times \text{dist}_{up}^{(j,k)}; S^{(j,k)} + \text{dist}_{up}^{(j,k)} \right] \quad (8)$$

$$M_u = \left[ S^{(j,k)} - \text{dist}_{down}^{(j,k)}; S^{(j,k)} - b_u \times \text{dist}_{down}^{(j,k)} \right] \quad (9)$$

$$\text{and } 0 < b_l < \dots < b_u < \dots < b_{c_q} < 1. \quad (10)$$

$\zeta$  is an increment parameter which modulates the thickness changes depending on the mass fraction change of the current iteration.  $\text{dist}_{up}^{(j,k)}$  and  $\text{dist}_{down}^{(j,k)}$  are the extreme discrepancies between the setpoint and the cells IED levels. Further details on the algorithm can be found in [15].

## 2.3 Implementation

The optimisation algorithm is implemented in the numerical programming and computation software Scilab [16]. The initial space filling is generated using the CAE software SFE CONCEPT [17, 18]. At each new iteration the model is updated automatically using this CAE software, i.e. SFE CONCEPT ensures the fully automated generation of a consistent geometry and realises then the modified finite element model. The cells' thickness are updated and the relevant cells are added or removed, the geometry is meshed and exported for simulation using the solver LS-Dyna [19].

## 3 Academic example, simplified pole impact

### 3.1 Problem definition

This example is taken from a collaborative project on topology optimisation for crashworthiness design of extruded cross-section [20]. The load case was defined by Ortmann *et al.* and is detailed in [10]. It is a simplified pole impact of a rocker and a seat cross-member (see Fig. 6). The rocker and cross-member have an initial velocity of 29 km/h and a mass of 85 kg is added at the end of the cross-member. The design task is to optimise the cross-section of the extruded rocker, while keeping the boundary fixed. The objective is to minimise the mass of the rocker while keeping the intrusion of the pole in the rocker under 75 mm and the maximum reaction force going through the cross-member under 48 kN.

The initial design is the empty cross-section with a boundary thickness of 3.5 mm. The mass is 2.801 kg, the intrusion is 69.03 mm and the maximum reaction force is 55.82 kN.

### 3.2 Topology optimisation with square space filling

The design space is filled with a square space filling (See Fig. 7). In the diagonal area of the cross-section, the square space filling is slightly distorted to ensure good connections between the cells and the boundary. The space filling is made of 65 cells. The thickness of the boundary is fixed to 1.75 mm. After running the optimisation, the best design found (See Fig. 8 and Fig. 9) has an intrusion of 74.5 mm, a mass of 1.764 kg and a maximum force of 45.2 kN.

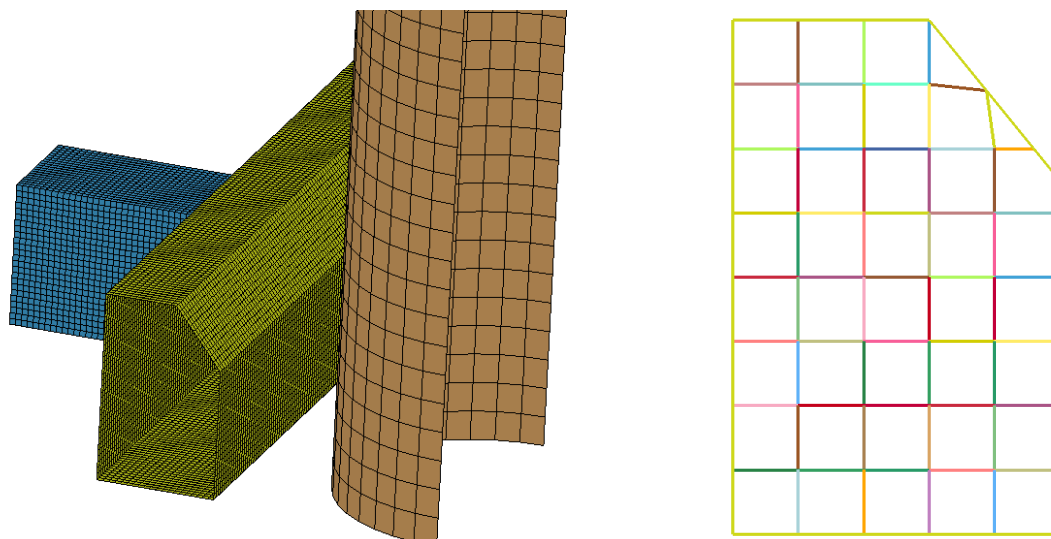


Figure 6: Load case, pole impact of rocker and seat Figure 7: Square space filling of the rocker cross-section.

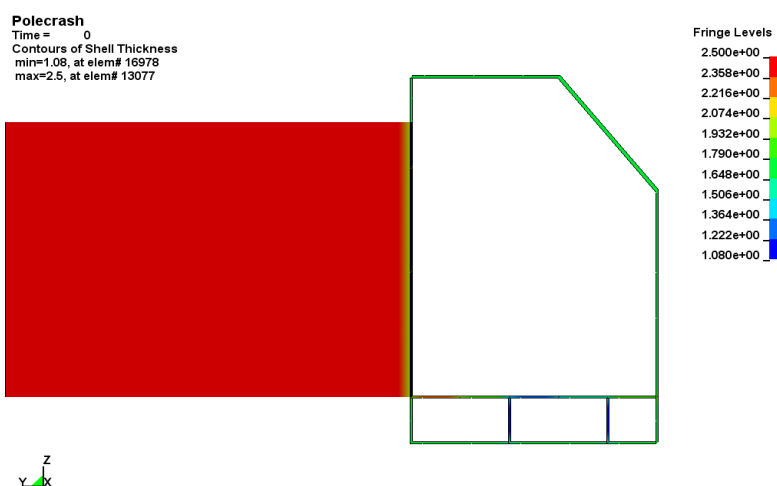


Figure 8: Best design for square space filling (thickness distribution).

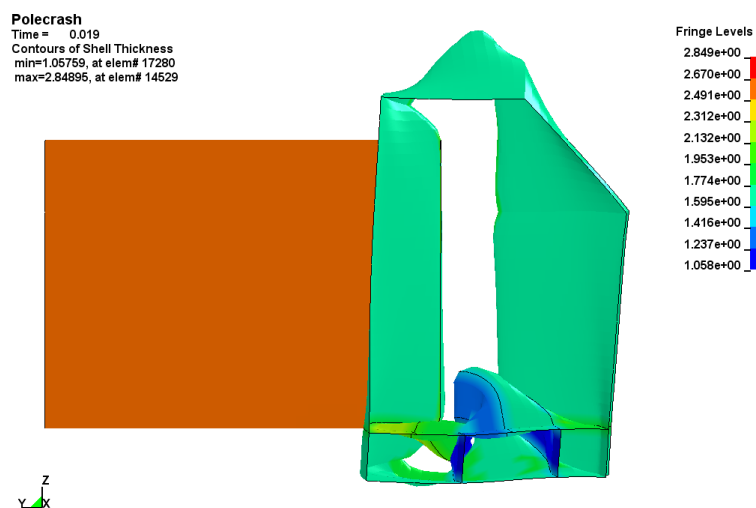


Figure 9: Best design for square space filling (maximum intrusion).

### 3.3 Topology optimisation with diagonal enriched space filling

An alternative space filling is also tested where the square space filling is enriched with diagonals (see Fig. 10). This new space filling is therefore made of 139 cells. The optimisation is run once again with this new space filling. The best design (See Fig. 11) has an intrusion of 71.4 mm, a mass of 1.951 kg and a maximum force of 46.3 kN. The topology is more complex than the one generated previously and the mass is higher. In this case, the square space filling gives a better result. It should be noted that this is not a general result. In other application examples not presented in this paper, the diagonal enriched space filling yields better results than the square space filling.

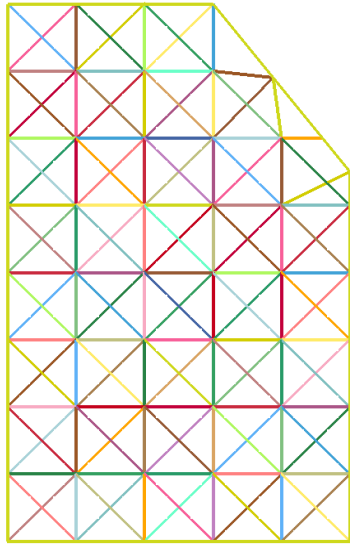


Figure 11: Diagonal enriched space filling of the rocker cross-section.

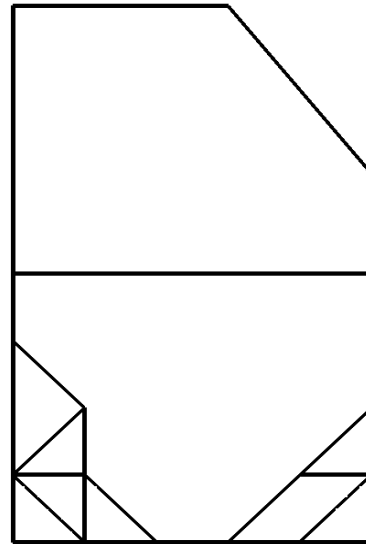


Figure 10: Best design for diagonal enriched space filling

### 3.4 Shape optimisation

To try and improve the design further, shape optimisation is performed on the results of the optimisation for the square space filling (see Fig. 8). The design parameters (see Fig. 12) are defined using the CAE software SFE CONCEPT. 20 parameters are defined with 12 translations and 8 thickness parameters. The optimisation is performed using LS-OPT [21] and genetic algorithms. The displacement constraint is lowered to  $d_{max}=70$  mm and the objective is now to minimise the maximum reaction force. Populations of 30 individuals are used. The best design (See Fig. 13) is found at iteration 24 with a displacement of 69.9 mm, a mass of 1.865 kg and a maximum force of 44.05 kN.

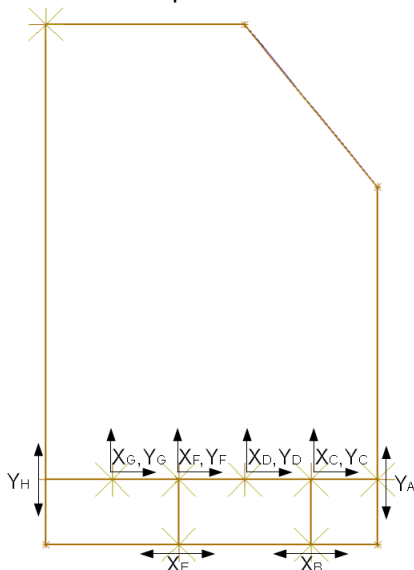


Figure 12: Parameters for shape optimisation.

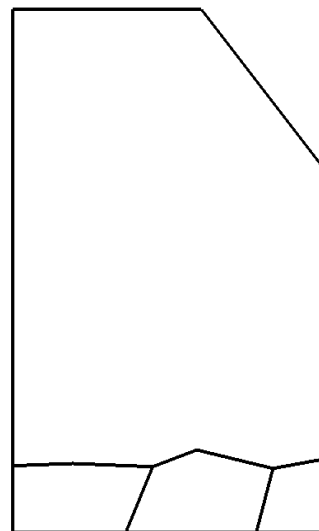


Figure 13: Best design cross-section.

The following table summarises the results for the different space fillings and for the shape optimisation. Using both the HCATWS to define a topology and a classic shape optimisation approach to finely tune the design allowed to improve mass and maximum reaction force while respecting the intrusion constraint.

	mass (kg)	intrusion (mm)	max-force (kN)
Initial design	2.801	69.03	55.82
Square filling, best	1.764	74.5	45.2
Diagonal filling, best	1.951	71.4	46.3
Shape opt. square filling	1.865	69.9	44.05

## 4 Industrial example, full vehicle pole impact

### 4.1 Problem definition

This second example is taken from the same collaborative project as previously [20]. Once again it is a pole impact but this time for a full vehicle. The design task remains the optimisation of a rocker cross-section, but this time with a much more complex geometry. The objective is to minimise the mass of the rocker while keeping the intrusion of the pole in the rocker under 170 mm. The initial rocker has an initial mass of 15.217 kg and an intrusion of 175 mm.

### 4.2 Topology optimisation with square space filling

The design space being more complex than the previous case, the space filling is not perfectly square. To follow the inclination of the cross-section boundary, parallelograms are used. Two space fillings are tested (See Fig. 14 and Fig. 15) using more or less of the initial cross-section of the rocker. In both cases, the space filling is slightly distorted when necessary to ensure connections with the boundary. The reduced space filling contains 45 cells while the extended space filling contains 71 cells.

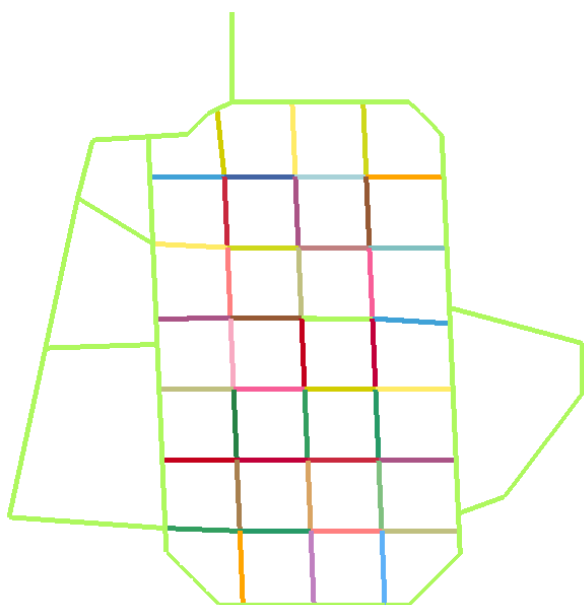


Figure 14: Reduced space filling.



Figure 15: Extended space filling.

The optimisation is run for both space fillings. The best design for the reduced space filling (see Fig. 16) has a mass of 14.969 kg with an intrusion of 169.9 mm. 15 of the original 45 cells define the topology. The best design for the extended space filling (see Fig. 17) has a mass of 13.768 kg with an intrusion of 169.0 mm. 31 of the original 71 cells define the topology. In both cases the mass has been reduced and the constraint is now respected.

LF\_Pfahl  
Time = 0  
Contours of Shell Thickness  
min=0.51, at elem# 67516  
max=3, at elem# 63904

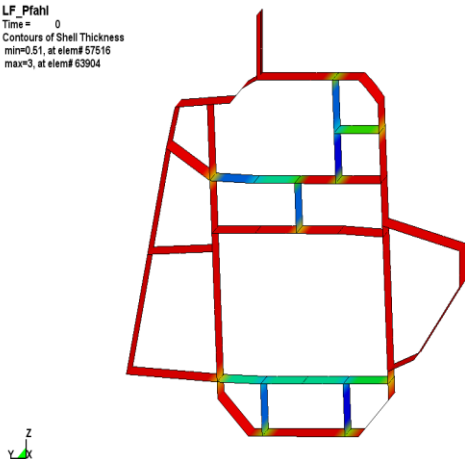


Figure 16: Best design for reduced space filling (thickness distribution).

LF\_Pfahl  
Time = 0  
Contours of Shell Thickness  
min=0.59, at elem# 58797  
max=3, at elem# 76365

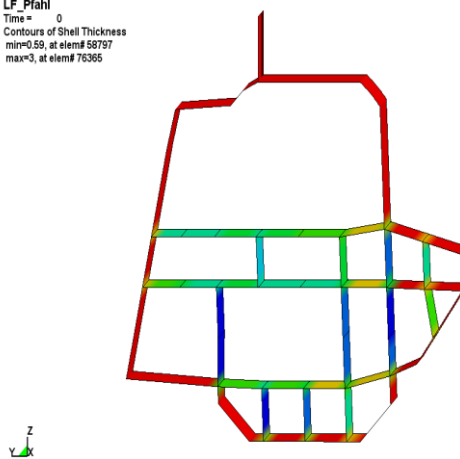


Figure 17: Best design for extended space filling (thickness distribution).

## 5 Summary

This paper presented a new method for topology optimisation in crashworthiness design. It uses the already established HCA and combines it with a ground structure made of thin walled macro elements. This approach allows to account for phenomena such as buckling and contact which can only be done with really small solid elements. It also has the advantage of directly generating thin-walled structures while other methods using 3D solid elements need some post-processing to interpret the results of the topology optimisation into a thin-walled structure.

Two application examples were detailed to showcase the potential of the method. The method still needs to be improved in order to be made more versatile and user friendly, but the early results are already encouraging.

## Acknowledgements

This research was funded partially by SFE GmbH and partially by Queen Mary University of London, which is acknowledged here. In particular the thanks go to SFE GmbH for providing not only the software SFE CONCEPT as a basis for the developments shown here, but also the generous support and discussions during the project. In addition the authors would like to thank the members of Crash-Topo project to allow them using the models and present the results detailed in the application examples. Eventually, the authors would like to thank ARUP UK for their generous support.

## References

- [1] Bendsøe, M.P.: "Optimal shape design as a material distribution problem", Structural Optimization, 1:193-202, 1989.
- [2] Volz, K.: "Physikalisch begründete Ersatzmodelle für die Crashtoptimierung von Karosseriestrukturen in frühen Projektphasen", PhD thesis, Technische Universität München, Germany, 2011.
- [3] Duddeck, F. and Volz, K.: "A new topology optimization approach for crashworthiness of passenger vehicles based on physically defined equivalent static loads", In International Crashworthiness Conference, Milano, Italy, 2012.
- [4] Christensen, J., Bastien, C. and Blundell, M.V.: "Effects of roof crush loading scenario upon body in white using topology optimisation", International Journal of Crashworthiness, 12(1):29-38, 2012.
- [5] Cavazzuti, M., Baldini, A., Bertocchi, E. Costi, D., Torricelli, E. and Moruzzi, P. : "High performance automotive chassis design: a topology optimization based approach", Structural and Multidisciplinary Optimization, 44:45-56, 2011.

- [6] Shin, M.K., Park, K.J., and Park, G.J.: "Optimization of structures with nonlinear behavior using equivalent loads", Computer Methods in Applied Mechanics and Engineering, 196:1154-1167, 2007.
- [7] Park, G.J.: "Equivalent static loads method for non linear static response structural optimization", In 9th LS-DYNA German User's Forum, Bamberg, Germany, 2010.
- [8] Park, G. J.: "Technical overview of the equivalent static loads method for non-linear static response structural optimization ", Structural and Multidisciplinary Optimization, 43(3):319-337, 2011.
- [9] Pedersen, C. B. W.: "On Topology design of frame structures for crashworthiness", PhD thesis, Technical University of Denmark, 2002.
- [10] Ortmann, C. and Schumacher, A.: "Graph and heuristic based topology optimization of crash loaded structures", Structural and Multidisciplinary Optimization, DOI 10.1007/s00158-012-0872-7, 2013.
- [11] Huang, X., Xie, Y. and Lu, G.: "Topology optimization of energy-absorbing structures", International Journal of Crashworthiness, 12(6):663-675, 2007.
- [12] Patel, N.: "Crashworthiness design using topology optimization", PhD thesis, University of Notre Dame, IL, USA, 2007.
- [13] Mozumder, C.: "Topometry optimization of sheet metal structures for crashworthiness design using hybrid cellular automata", PhD thesis, University of Notre Dame, IL, USA, 2010.
- [14] Bochenek, B. and Tajs-Zielińska, K.: "Local rules of cellular automata for generating optimal topologies in structural design", In ECCM 2010, IV European Conference on Computational Mechanics, Paris, France, 2010.
- [15] Hunkeler, S.: "Topology Optimisation in Crashworthiness Design via Hybrid Cellular Automata for Thin Walled Structures", PhD thesis, Queen Mary University of London, to be published.
- [16] The Scilab Consortium. Scilab. [www.scilab.org](http://www.scilab.org).
- [17] SFE GmbH, Berlin, Germany. SFE CONCEPT Ver 4.2.2.3, Reference Manual, 2009.
- [18] Zimmer, H.: „Target conflicts during the early design phase of CAE-driven vehicle development“, In NAFEMS Seminar "Concept Design Driven by Simulation", Wiesbaden, Germany, 2013.
- [19] Livermore Software Technology Corporation, Livermore, USA. LS-DYNA - Theory manual,2006.
- [20] Research project (Nov 2009-11) "Methodical and Software-Technical Implementation of Topology Optimization for Crash-stressed Vehicle Structures" funded by the German Federal Ministry of Education and Research (BMBF) with the German partners ASCS (Automotive Simulation Center Stuttgart), Dynamore GmbH, HAW Hamburg, SFE GmbH. [http://www.asc-s.de/dokumente/asc\(s\)\\_Project\\_Crash-Topo.pdf](http://www.asc-s.de/dokumente/asc(s)_Project_Crash-Topo.pdf).
- [21] Livermore Software Technology Corporation, Livermore, USA. LS-OPT User's Manual, Version 4.2, 2012.